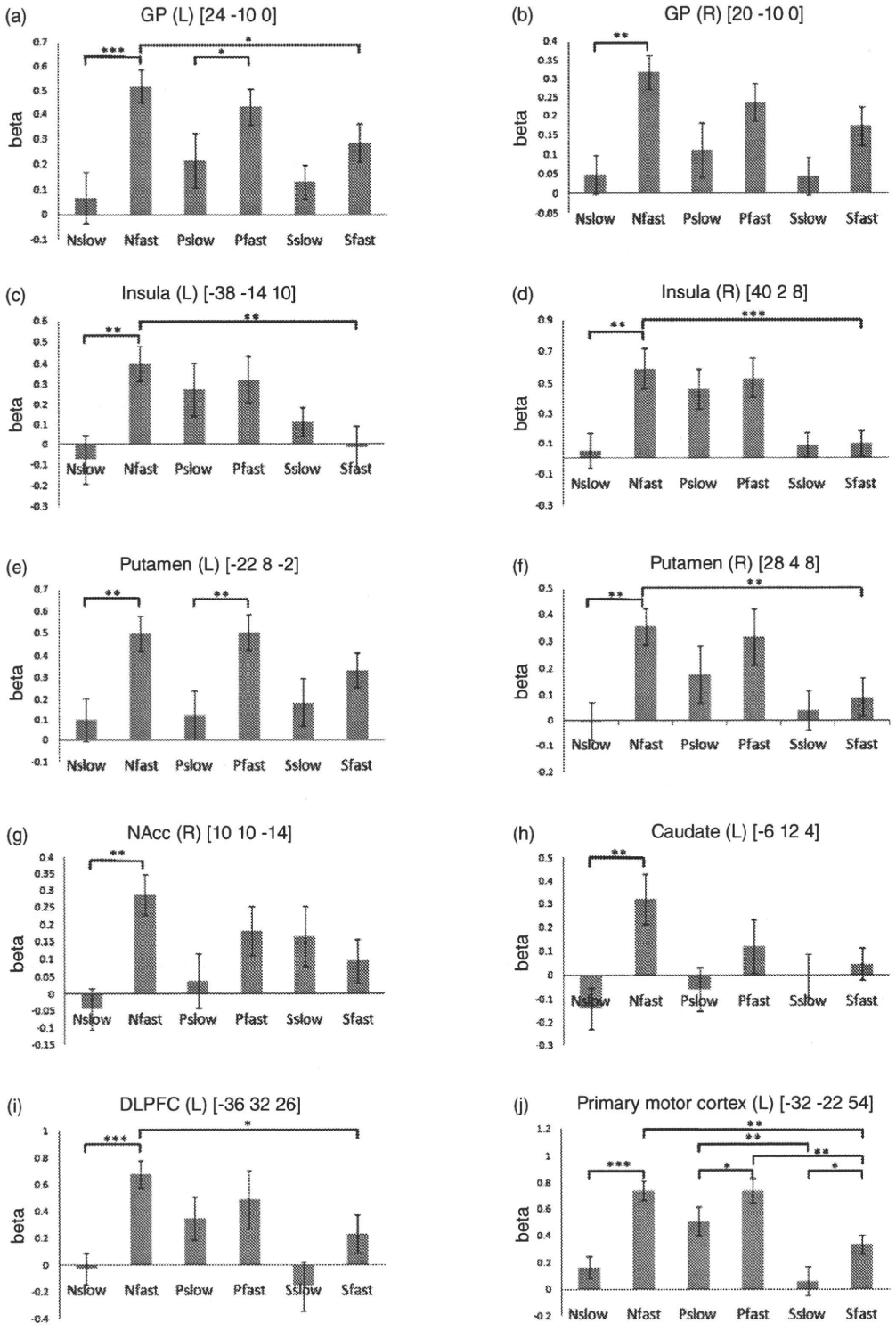

Figure 1. The mean beta values for the peak activation categorized by drug and reaction time type for the defined regions-of-interest. $*P < 0.05$, $**P < 0.01$, $***P < 0.001$. Error bars show SEM. DLPFC, dorsolateral prefrontal cortex; GP, globus pallidus; L, left; NAcc, nucleus accumbens; R, right.

These results might partly come from the duration of drug administration because sufficient antidepressive effects of SSRI are not apparent normally until after 3–6 weeks of treatment. The increase in 5-HT produced by a single administration of SSRI not only stimulates the postsynaptic 5-HT receptors but also stimulates the somatodendritic inhibitory 5-HT_{1A} autoreceptors and presynaptic 5-HT_{1B} and 5-HT_{1D} autoreceptors. This varied activity could produce a net reduction in the activity of the 5-HT system.[32] Long-term treatment with SSRI induces desensitization/internalization of 5-HT autoreceptors, and this could lead to the downregulation of some postsynaptic receptors, such as the 5-HT_{2A} and 5-HT_{2C} subtypes. The end result of this process is thought to be a net activation of the 5-HT system.[32] Our results may partly arise from a net reduction of serotonin function by 5-HT autoreceptors produced by acute paroxetine administration.

We should briefly mention a relatively strong affinity of paroxetine for the norepinephrine transporter, $K_D = 40 \pm 2$ nmol[23] and muscarine receptor, $K_i = 72 \pm 3$ nmol/L,[22] but it is beyond the scope of the present study to examine the effects of paroxetine on these pathways.

In conclusion, paroxetine single acute administration diminished brain activity induced by motivation in healthy subjects. Our results may partially explain clinically observed decreased motivation seen in patients with relatively mild symptoms taking an initial paroxetine tablet dose of 10 or 20 mg for the first time. Further research is needed to clarify the effects of SSRI on brain activity with respect to cognitive and motor functions.

ACKNOWLEDGMENTS

We gratefully acknowledge the contributions of the members of the Tamagawa University Brain Science Institute. This work was supported by Grants-in-Aid for Scientific Research #19790838 and #18300275 for T. M. and Tamagawa University Global Center of Excellence (GCOE) program from the Japanese Ministry of Education, Culture, Sports, Science and Technology (MEXT).

REFERENCES

1. American Psychiatric Association. *Diagnostic and Statistical Manual of Mental Disorders DSM-IV-TR*, 4th edn. American Psychiatric Association, Washington, DC, 1994.
2. Naranjo CA, Tremblay LK, Busto UE. The role of the brain reward system in depression. *Prog. Neuropsychopharmacol. Biol. Psychiatry* 2001; 25: 781–823.
3. Treadway MT, Buckholtz JW, Schwartzman AN, Lambert WE, Zald DH. Worth the 'EEfRT'? The effort expenditure for rewards task as an objective measure of motivation and anhedonia. *PLoS ONE* 2009; 4: e6598.
4. Opbroek A, Delgado PL, Laukes C *et al.* Emotional blunting associated with SSRI-induced sexual dysfunction. Do SSRIs inhibit emotional responses? *Int. J. Neuropsychopharmacol.* 2002; 5: 147–151.
5. Prince J, Cole V, Goodwin GM. Emotional side-effects of selective serotonin reuptake inhibitors: qualitative study. *Br. J. Psychiatry* 2009; 195: 211–217.
6. Shelton RC, Tomarken AJ. Can recovery from depression be achieved? *Psyichiatr. Serv.* 2001; 52: 1469–1478.
7. Dickinson A, Balleine B. Motivational control of goal-directed action. *Anim. Learn. Behav.* 1994; 22: 1–18.
8. Roesch MR, Olson CR. Neutral activity related to reward value and motivation in primate frontal cortex. *Science* 2004; 304: 307–310.
9. Loubinoux I, Pariente J, Boulanouar K *et al.* A single dose of the serotonin neurotransmission agonist paroxetine enhances motor output: double-blind, placebo-controlled, fMRI study in healthy subjects. *NeuroImage* 2002; 15: 26–36.
10. Loubinoux I, Pariente J, Rascol O, Celsis P, Chollet F. Selective serotonin reuptake inhibitor paroxetine modulates motor behavior through practice. A double-blind, placebo-controlled, multi-dose study in healthy subjects. *Neuropsychologia* 2002; 40: 1815–1821.
11. Wingen M, Kuypers KP, van de Ven V, Formisano E, Ramaekers JG. Sustained attention and serotonin: a pharmaco-fMRI study. *Hum. Psychopharmacol.* 2008; 23: 221–230.
12. Del-Ben CM, Deakin JFW, Mckie S *et al.* The effect of citalopram pretreatment on neuronal responses to neuropsychological tasks in normal volunteers: an fMRI Study. *Neuropsychopharmacology* 2005; 30: 1724–1734.
13. McCabe C, Mishor Z, Cowen PJ, Harmer CJ. Diminished neural processing of aversive and rewarding stimuli during selective serotonin reuptake inhibitor treatment. *Biol. Psychiatry* 2010; 67: 439–455.
14. Barnhart WJ, Makela EH, Latocha MJ. SSRI-induced apathy syndrome: a clinical review. *J. Psychiatr. Pract.* 2004; 10: 196–199.
15. Hasler G, Drevets WC, Manji HK, Charney DS. Discovering endophenotypes for major depression. *Neuropsychopharmacology* 2004; 29: 1765–1781.
16. Beer MH, Porter RS, Jones TV. *The Merck Manual of Diagnosis and Therapy*, 18th edn. Merck Sharp & Dohme Corp, Whitehouse Station, 2006.
17. Knutson B, Adams CM, Fong GW, Hommer D. Anticipation of increasing monetary reward selectively recruits nucleus accumbens. *J. Neurosci.* 2001; 21 (RC159): 1–5.

18. Dillon DG, Holmes AJ, Jahn AL, Bogdan R, Wald LL, Pizzagalli DA. Dissociation of neural regions associated with anticipatory versus consummatory phases of incentive processing. *Psychophysiology* 2008; **45**: 36–49.
19. Knutson B, Taylor J, Kaufman M, Peterson R, Glover G. Distributed neural representation of expected value. *J. Neurosci.* 2005; **25**: 4806–4812.
20. Scott DJ, Stohler CS, Egnatuk CM, Wang H, Koeppe RA, Zubieta JK. Individual differences in reward responding explain placebo-induced expectations and effects. *Neuron* 2007; **55**: 325–336.
21. Owens MJ, Morgan WN, Plott SJ, Nemeroff CB. Neurotransmitter receptor and transporter binding profile of antidepressants and their metabolites. *J. Pharmacol. Exp. Ther.* 1997; **283**: 1305–1322.
22. Owens MJ, Knight DL, Nemeroff CB. Second-generation SSRIs: human monoamine transporter binding profile of escitalopram and R-fluoxetine. *Biol. Psychiatry* 2001; **50**: 345–350.
23. Tatsumi M, Groshan K, Blakely RD, Richelson E. Pharmacological profile of antidepressants and related compounds at human monoamine transporters. *Eur. J. Pharmacol.* 1997; **340**: 249–258.
24. Irie H, Fujita M, Inokawa Y, Narita H. Phase 1 clinical study of paroxetine HCl (Study 3): Pharmacokinetics after single oral administration of paroxetine HCl 10,20 and 40 mg to healthy adult male volunteers. *Jpn. Pharmacol. Ther.* 2000; **28**: S47–S68 (in Japanese).
25. Meyer JH, Wilson AA, Sagrati S *et al.* Serotonin transporter occupancy of five selective serotonin reuptake inhibitors at different doses: an [11C]DASB positron emission tomography study. *Am. J. Psychiatry* 2004; **161**: 826–835.
26. Suhara T, Takano A, Sudo Y *et al.* High levels of serotonin transporter occupancy with low-dose clomipramine in comparative occupancy study with fluvoxamine using positron emission tomography. *Arc. Gen. Psychiatry* 2003; **60**: 386–391.
27. Ashburner J, Friston KJ. Nonlinear spatial normalization using basis functions. *Hum. Brain Mapp.* 1999; **7**: 254–266.
28. Tanaka S, Doya K, Okada G, Ueda K, Okamoto Y, Yamawaki S. Prediction of immediate and future rewards differentially recruits cortico-basal ganglia loops. *Nat. Neurosci.* 2004; **7**: 887–893.
29. Knutson B, Fong GW, Adams CM, Varner JL, Hommer D. Dissociation of reward anticipation and outcome with event-related fMRI. *NeuroReport* 2001; **12**: 3683–3687.
30. Carrillo-de-la-Peña MT, Galdo-Álvarez S, Lastra-Barreira C. Equivalent is not equal: primary motor cortex (MI) activation during motor imagery and execution of sequential movements. *Brain Res.* 2008; **1226**: 134–143.
31. Critchley HD, Mathias CJ, Dolan RJ. Neural activity in the human brain relating to uncertainty and arousal during anticipation. *Neuron* 2001; **29**: 537–545.
32. Cools R, Roberts AC, Robbins TW. Serotoninergic regulation of emotional and behavioural control processes. *Trends Cogn. Sci.* 2008; **12**: 31–40.

Behavioral/Systems/Cognitive

Contribution of Dopamine D1 and D2 Receptors to Amygdala Activity in Human

Hidehiko Takahashi,[1,3] Harumasa Takano,[1] Fumitoshi Kodaka,[1] Ryosuke Arakawa,[1] Makiko Yamada,[1] Tatsui Otsuka,[1] Yoshiyuki Hirano,[2] Hideyuki Kikyo,[1] Yoshiro Okubo,[4] Motoichiro Kato,[5] Takayuki Obata,[2] Hiroshi Ito,[1] and Tetsuya Suhara[1]

Departments of [1]Molecular Neuroimaging and [2]Biophysics, Molecular Imaging Center, National Institute of Radiological Sciences, Chiba 263-8555 Japan, [3]Precursory Research for Embryonic Science and Technology, Japan Science and Technology Agency, Saitama, 332-0012, Japan, [4]Department of Neuropsychiatry, Nippon Medical School, Tokyo 113-8603, Japan, and [5]Department of Neuropsychiatry, Keio University School of Medicine, Tokyo 160-8582, Japan

Several animal studies have demonstrated functional roles of dopamine (DA) D1 and D2 receptors in amygdala activity. However, the contribution of DA D1 and D2 receptors to amygdala response induced by affective stimuli in human is unknown. To investigate the contribution of DA receptor subtypes to amygdala reactivity in human, we conducted a multimodal in vivo neuroimaging study in which DA D1 and D2 receptor bindings in the amygdala were measured with positron emission tomography (PET), and amygdala response induced by fearful faces was assessed by functional magnetic resonance imaging (fMRI) in healthy volunteers. We used multimodality voxelwise correlation analysis between fMRI signal and DA receptor binding measured by PET. DA D1 binding in the amygdala was positively correlated with amygdala signal change in response to fearful faces, but DA D2 binding in the amygdala was not related to amygdala signal change. DA D1 receptors might play a major role in enhancing amygdala response when sensory inputs are affective.

Introduction

The amygdala plays a central role in processing affective stimuli, and in particular, threatening stimuli in the brain (LeDoux, 2000). The amygdala receives a moderate innervation of dopaminergic fibers (Asan, 1998), and both dopamine (DA) D1 and D2 receptors are expressed in this region (Ito et al., 2008), although the latter exhibit lower expression (Scibilia et al., 1992). DA release in the amygdala is increased in response to stress (Inglis and Moghaddam, 1999). It has been shown in animal studies that DA potentiates the response of the amygdala by augmenting excitatory sensory input and attenuating inhibitory prefrontal input to the amygdala (Rosenkranz and Grace, 2002). Systemic and local applications into the amygdala of D1 agonist and antagonist are known to potentiate and decrease fear response in animals, respectively. Although some studies reported that applications of D2 agonist and antagonist induced similar effects, the results were less consistent compared with D1-mediated effects (for review, see Pezze and Feldon, 2004; de la Mora et al., 2009).

A human functional magnetic resonance imaging (fMRI) study reported that doparminergic drug therapy such as levodopa or DA agonists partially restored amygdala response due to emotional task in Parkinson's disease patients who showed no significant amygdala response during drug-off states (Tessitore et al., 2002). In addition, another fMRI study of healthy volunteers has demonstrated that amphetamine potentiated the response of the amygdala during an emotional task (Hariri et al., 2002). More recently, Kienast et al. (2008) reported that dopamine storage capacity in human amygdala, measured with 6-[^{18}F]fluoro-L-DOPA positron emission tomography (PET), was positively correlated with functional magnetic resonance imaging (fMRI) signal changes in amygdala. However, the contribution of DA D1 and D2 receptors to amygdala response induced by affective stimuli is unknown in human. To investigate the relation between amygdala reactivity and dopamine receptor subtype, we conducted a multimodal in vivo neuroimaging study in which DA D1 and D2 receptor bindings in the amygdala were measured with PET, and amygdala response by novel faces with either neutral or fearful expression was assessed with fMRI. Based on animal pharmacological studies, we hypothesized that D1, but not D2 receptors, would predict amygdala response.

Received Nov. 17, 2009; revised Jan. 8, 2010; accepted Jan. 8, 2010.

This study was supported by a consignment expense for Molecular Imaging Program on "Research Base for PET Diagnosis" from the Ministry of Education, Culture, Sports, Science and Technology. Takanori Kochiyama and Yoko Ikoma are greatly acknowledged for her comments. We thank K. Tanimoto and T. Shiraishi for their assistance in performing the PET experiments at the National Institute of Radiological Sciences. We also thank Y. Fukushima, K. Suzuki, and I. Izumida of the National Institute of Radiological Sciences for their help as clinical research coordinators.

Correspondence should be addressed to Hidehiko Takahashi, Department of Molecular Neuroimaging, National Institute of Radiological Sciences, 9-1, 4-chome, Anagawa, Inage-ku, Chiba, Chiba 263-8555, Japan. E-mail: hidehiko@nirs.go.jp.

DOI:10.1523/JNEUROSCI.5689-09.2010

 0270-6474/10/303043-05$15.00/0

Materials and Methods

Subjects

Twenty-one male volunteers [mean age 23.1 ± (SD) 3.6 years] were studied. They did not meet the criteria for any psychiatric disorder based on unstructured psychiatric screening interviews. None of the controls were taking alcohol at the time, nor did they have a history of psychiatric disorder, significant physical illness, head injury, neurological disorder, or alcohol or drug dependence. All subjects were right-handed according to the Edinburgh Handedness Inventory. All subjects underwent MRI to rule out cerebral anatomic abnormalities. After complete explanation of the study,

written informed consent was obtained from all subjects, and the study was approved by the Ethics and Radiation Safety Committee of the National Institute of Radiological Sciences, Chiba, Japan.

fMRI procedure

Stimulus materials were taken from the Karolinska Directed Emotional Faces (KDEF) (Lundqvist et al., 1998). Thirty neutral and 30 fear faces were used, with half of them being male faces. The pictures were projected via a computer and a telephoto lens onto a screen mounted on a head-coil. The experimental design consisted of 5 blocks for each of the 2 conditions (neutral, fear) interleaved with 21 s rest periods. The order of presentation for the 2 conditions (neutral and fear) was randomized. During the baseline condition, subjects viewed a crosshair pattern projected to the center of the screen. In each 21 s block, 6 different faces of the same emotional class were presented for 3.5 s each. During the scans, the subjects were instructed to judge the gender of each face using selection buttons.

fMRI scanning

The images were acquired with a 3.0 Tesla Excite system (General Electric). Functional images of 126 volumes were acquired with T2*-weighted gradient echo planar imaging sequences sensitive to the blood oxygenation level-dependent (BOLD) contrast. Each volume consisted of 40 transaxial contiguous slices with a slice thickness of 3 mm to cover almost the whole brain (flip angle, 90°; echo time, 50 ms; repetition time, 3500 ms; matrix, 64 × 64; field of view, 24 × 24 cm).

Analysis of fMRI data

Data analysis was performed with the statistical parametric mapping software package (SPM2) (Wellcome Department of Cognitive Neurology, London, UK) running with MATLAB (MathWorks). All volumes were realigned to the first volume of each session to correct for subject motion and were spatially normalized to the standard space defined by the Montreal Neurological Institute (MNI) template. After normalization, all scans had a resolution of $2 \times 2 \times 2$ mm^3. Functional images were spatially smoothed with a three-dimensional isotropic Gaussian kernel (full-width at half-maximum of 8 mm). Low-frequency noise was removed by applying a high-pass filter (cutoff period = 128 s) to the fMRI time series at each voxel. A temporal smoothing function was applied to the fMRI time series to enhance the temporal signal-to-noise ratio. Significant hemodynamic changes for each condition were examined using the general linear model with boxcar functions convolved with a hemodynamic response function. Statistical parametric maps for each contrast of t-statistic were calculated on a voxel-by-voxel basis.

We assessed the contrasts of fear and neutral minus baseline (F&N-B). A random effects model, which estimates the error variance for each condition across the subjects, was implemented for group analysis. The contrast images were obtained from single-subject analysis and entered into the group analysis. A one-sample t test was applied to determine group response for each effect. Significant amygdala activations were identified if they reached the extent threshold of $p < 0.05$ corrected for multiple comparisons, with a height threshold of $p < 0.001$, uncorrected.

PET scanning

After the fMRI session, each participant underwent PET scanning. The interval between fMRI session and PET scan was 3–5 h. PET studies were performed on ECAT EXACT HR+ (CTI-Siemens). The system provides 63 planes and a 15.5 cm field of view. To minimize head movement, a head fixation device (Fixster) was used. A transmission scan for attenuation correction was performed using a germanium 68–gallium 68 source. Acquisitions were done in three-dimensional mode with the interplane septa retracted. For evaluation of D1 receptors, a bolus of 219.7 ± 6.9 MBq of [^{11}C]SCH23390 with specific radioactivities (95.7 ± 35.5 GBq/μmol) was injected intravenously from the antecubital vein with a 20 ml saline flush. For evaluation of extrastriatal DA D2 receptors, a bolus of 218.1 ± 14.7 MBq of [^{11}C]FLB457 with high specific radioactivities (221.6 ± 94.9 GBq/μmol) was injected in the same way. Dynamic scans were performed for 60 min for [^{11}C]SCH23390 and 90 min for [^{11}C]FLB457 immediately after the injection. All emission scans were reconstructed with a Hanning filter cutoff frequency of 0.4 (full-width at half-maximum, 7.5 mm). MRI was performed on Gyroscan NT (Philips Medical Systems) (1.5 T). T1-weighted images of the brain were obtained for all subjects. Scan parameters were 1-mm-thick, three-dimensional T1 images with a transverse plane (repetition time/echo time, 19/10 ms; flip angle, 30°; scan matrix, 256 × 256 pixels; field of view, 256 × 256 mm; and number of excitations, 1).

Quantification of DA D1 and D2 receptors

Quantitative analysis was performed using the three-parameter simplified reference tissue model (Lammertsma and Hume, 1996; Olsson et al., 1999). The cerebellum was used as a reference region because it has been shown to be almost devoid of DA D1 and D2 receptors (Farde et al., 1987; Olsson et al., 1999; Suhara et al., 1999). The model provides an estimation of the binding potential ($BP_{ND\ (nondisplaceable)}$) (Innis et al., 2007), which is defined by the following equation: $BP_{ND} = k_3/k_4 = f_2 B_{max}/\{K_d [1 + \Sigma_i F_i/K_{di}]\}$, where k_3 and k_4 describe the bidirectional exchange of tracer between the free compartment and the compartment representing specific binding, f_2 is the "free fraction" of nonspecifically bound radioligand in brain, B_{max} is the receptor density, K_d is the equilibrium dissociation constant for the radioligand, and F_i and K_{di} are the free concentration and dissociation constant of competing ligands, respectively (Lammertsma and Hume, 1996). Tissue concentrations of the radioactivities of [^{11}C]SCH23390 and [^{11}C]FLB457 were obtained from regions of interest (ROIs) defined on PET images of summated activity for 60 min and 90 min, respectively, with reference to the individual MRIs coregistered on summated PET images and the brain atlas. Given our hypothesis of amygdala activation during viewing novel neutral and fearful faces, ROIs were set on the bilateral amygdala. The method for defining the boundaries of the amygdala was adapted from previously described methods (Kates et al., 1997; Convit et al., 1999). In short, the amygdala ROIs consisted of three axial slices. The anterior and posterior boundaries were identified at the level of the optic chiasm and the temporal horn of the lateral ventricle, respectively. The superior and inferior-lateral boundaries were identified at the level of the mammalian body and the temporal lobe white matter and extension of the temporal horn, respectively. We also created parametric images of BP_{ND} using the basis function method (Gunn et al., 1997) to conduct voxelwise SPM analysis in addition to ROI analysis.

Statistical analysis

ROI correlation analysis. Estimates of percentage signal change of fear vs baseline condition were extracted from the amygdala for each participant using the MarsBaR toolbox (Brett et al., 2002). The bilateral amygdala ROIs were defined from the WFU-Pickatlas SPM tool (Maldjian et al., 2003) with the aal atlas (Tzourio-Mazoyer et al., 2002). Correlation between BP_{ND} of [^{11}C]SCH23390 and [^{11}C]FLB457 in the bilateral amygdala and bilateral amygdala fMRI signal change were calculated using SPSS.

Confirmatory SPM correlation analysis. Parametric images of BP_{ND} of [^{11}C]SCH23390 and [^{11}C]FLB457 were analyzed using SPM2. Exactly the same image preprocessings of normalization and smoothing that were used in fMRI data analysis were applied to parametric images of BP_{ND}. To conduct multimodality voxelwise correlation analysis between the BOLD signal and DA receptor binding, we used the biological parametric mapping toolbox for SPM (Casanova et al., 2007). Significant clusters were identified if they reached the extent threshold of $p < 0.05$ corrected for multiple comparisons, with a height threshold of $R > 0.6$ ($p < 0.003$ uncorrected).

Results

Since the face pictures consisted of Caucasian faces (racial outgroup), even novel neutral faces produced amygdala response in several participants (Hart et al., 2000; Schwartz et al., 2003), leading to a blunted contrast of fear minus neutral. Therefore, we combined neutral and fear conditions and used F&N-B contrast for analyses. Group analysis of F&N-B contrast revealed significant bilateral amygdala responses [right amygdala (26, 0, −26), $t = 4.43$, 93 voxels, left amygdala (−20, −2, −26), $Z = 4.96$, 101

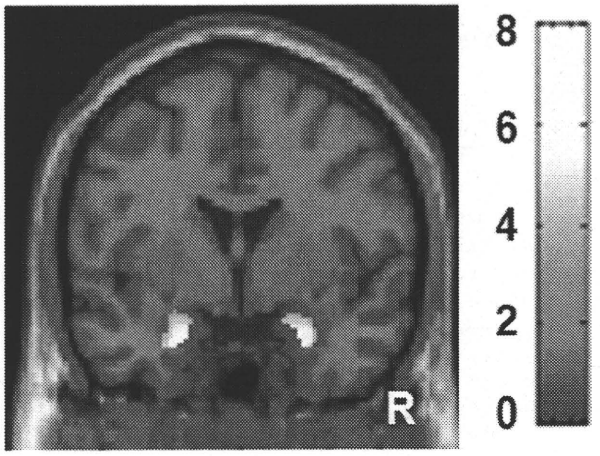

Figure 1. Images showing brain response induced by fear and neutral minus baseline condition. Bilateral amygdala responses are shown. The bar shows the range of the t-value. R indicates right.

voxels] (Fig. 1). The mean BP_{ND} of [^{11}C]SCH23390 in the right and left amygdala were 0.38 ± 0.08 and 0.39 ± 0.11, respectively. The mean BP_{ND} of [^{11}C]FLB457 in the right and left amygdala were 2.49 ± 0.50 and 2.50 ± 0.44, respectively.

Correlation analysis of biological parametric mapping revealed that the BP_{ND} value of [^{11}C]SCH23390 in the right amygdala was positively correlated with the BOLD signals in the right amygdala of F&N-B contrast [peak (28, 2, −28), 24 voxels] (Fig. 2A). ROIs analysis also revealed a similar significant correlation ($r = 0.59$, $p = 0.005$) in the right amygdala (Fig. 2B), but not in the left amygdala ($r = 0.18$, $p = 0.43$). According to biological parametric mapping analysis, the BP_{ND} value of [^{11}C]FLB457 in the amygdala was not correlated with BOLD signals in the amygdala of F&N-B contrast. ROIs analysis showed that right and left amygdala D2 binding was not correlated with the BOLD signals in the right ($r = 0.26$, $p = 0.27$) and left amygdala ($r = 0.28$, $p = 0.23$), respectively. Both biological parametric mapping analysis and ROIs analysis showed that D1 binding in the right and left amygdala was not correlated with D2 binding in the right ($r = 0.24$, $p = 0.30$) and left amygdala ($r = 0.16$, $p = 0.49$), respectively. We used anatomically defined ROIs of the amygdala rather than functional ROIs defined by fMRI in the ROI correlation analysis because it is difficult to place functionally defined ROIs on individual PET data. Anatomically defined ROIs of the amygdala were larger than functionally defined amygdala ROIs. This fact was advantageous in increasing the signal-to-noise ratio in the PET analysis, but led to blunted BOLD signal changes in the amygdala. However, BOLD signal changes derived from both ROI methods were highly correlated with each other. For example, very high correlation ($r = 0.80$, $p < 0.001$) was observed in the right amygdala. Thus, regardless of ROI definition method, we obtained similar results from ROI correlation analyses between BOLD signal changes and DA receptor binding in the amygdala.

Discussion

Using a multimodality in vivo neuroimaging approach, we first directly compared amygdala DA D1 and D2 receptor bindings, indices of receptor availability, with amygdala response evoked by novel or fearful stimuli in human. We found that DA D1 receptors, but not D2 receptors, predicted amygdala response induced by novel facial stimuli with either neutral or fearful expression. Our findings broaden our knowledge about dopaminergic transmission in amygdala response beyond the recent study (Kienast et al., 2008) that elucidated the relation between presynaptic dopamine synthesis and amygdala reactivity.

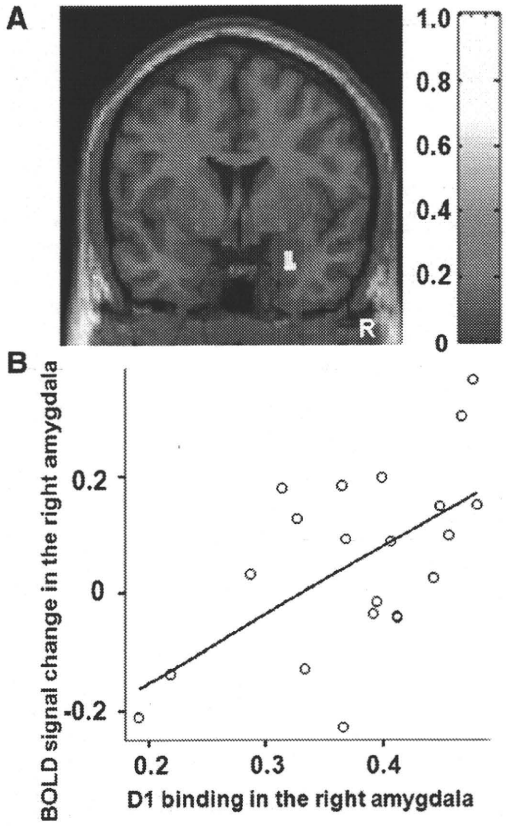

Figure 2. A, SPM correlation analysis revealed significant positive linear correlations between D1 binding in the right amygdala and right amygdala signal change. The bar shows the range of the correlation coefficient. B, ROI correlation analysis also revealed similar correlations. R indicates right.

Human neuroimaging studies reported that DA potentiated amygdala response evoked by affective stimuli (Hariri et al., 2002; Tessitore et al., 2002). In rat studies, Rosenkranz and Grace (2002) demonstrated that DA enhances the response of the amygdala by augmenting excitatory sensory input via DA D2 receptor stimulation and attenuating inhibitory prefrontal input to the amygdala through DA D1 receptor stimulation. More recently, it was demonstrated that both D1 and D2 receptor stimulations directly enhanced the excitability of amygdala projection neurons via postsynaptic mechanism (Rosenkranz and Grace, 2002; Kröner et al., 2005; Yamamoto et al., 2007). Amygdala projection neurons are under inhibitory control by GABAergic interneurons (Royer et al., 1999). Both projection neurons and interneurons in the amygdala express DA D1 and D2 receptors (Rosenkranz and Grace, 1999). It has been shown that DA and D1 receptor stimulation augments interneuron excitability and increases the frequency of IPSC in amygdala projection neurons (Kröner et al., 2005). This is a counterintuitive result, considering the fact that DA disinhibits amygdala response in vivo. However, Marowsky et al. (2005) found that a subpopulation of amygdala interneurons (paracapsular intercalated cells), located between the major input and output stations of amygdala, is suppressed by DA through D1 receptor stimulation. DA D2 receptors also play a role in disinhibiting amygdala response by decreasing inhibi-

tion onto projection neurons and increasing inhibition onto interneurons (Bissière et al., 2003).

Although detailed examination of subnuclei of the amygdala is difficult in this imaging method, the dorsal portion of the amygdala roughly corresponds to the central nuclei of amygdala (CeA) and the ventral portion of the amygdala corresponds to the basolateral nuclei of amygdala (BLA) and intercalated cell masses (ICM) (Whalen et al., 2009). The amygdala clusters identified both in fMRI task effect analysis and in correlation analysis between D1 binding and amygdala reactivity were located in the ventral portion of the amygdala. Thus, our findings seem to mainly reflect BLA and ICM properties. It is worth mentioning that the highest density of D1 receptors within the amygdala was found in the ICM, followed by BLA, and the expression of D1 receptors is low in CeA (de la Mora et al., 2009; Muly et al., 2009). In contrast, D2 receptors are mainly distributed in CeA (de la Mora et al., 2009). Both D1 and D2 receptors are expressed both postsynaptically in dendrites and presynaptically in axon terminals (Pinto and Sesack, 2008; Muller et al., 2009; Muly et al., 2009), but D1 receptors in BLA are mainly expressed in the dendrites, indicating that DA directly modulates the excitability of BLA projection neurons and interneurons. At the same time, DA also acts on presynaptic D1 receptors to increase the probability of neurotransmitter release from glutamatergic terminals (Muly et al., 2009). Thus, the net DA effect on D1 receptors in the amygdala is a complex mixture of post- and presynaptic actions at several sites.

Although both DA D1 and D2 receptors contribute to potentiating amygdala response via various mechanisms as described above, our finding suggested that DA D1 receptors play a major role in the overall potentiation of amygdala response. At a behavioral level, previous animal studies repeatedly reported that D1 agonist and antagonist applications into the amygdala potentiated and decreased fear response, respectively. However, the effects of D2 agonist/antagonist on fear response have not been well established (Pezze and Feldon, 2004; de la Mora et al., 2009). Thus, the current finding could be regarded as being consistent with previous behavioral pharmacological studies. The combination of PET molecular imaging and fMRI seems to represent a powerful approach for understanding molecular functions in system neuroscience. However, this study has several limitations. First, current PET techniques for human do not have enough spatial resolution to distinguish subnuclei of the amygdala. Although analysis of parametric images of BP_{ND} has become well established (Gunn et al., 1997) and is used in many [^{11}C]SCH23390 and [^{11}C]FLB457 studies (Cervenka et al., 2006; Takahashi et al., 2008; Karlsson et al., 2009; McNab et al., 2009), a very small region or a single voxel is susceptible to partial volume effect. Thus, it is recommended that parametric image analysis should be used in combination with ROI analysis. At the same time, current results merit further investigation with a higher resolution PET scanner. Second, PET imaging cannot tell us the exact location of DA receptors expressed in projection neurons and interneurons. Future animal studies or in vitro studies would complement our findings to determine which D1 receptor-mediated mechanism is most responsible for the overall amygdala response. Third, differences in DA receptor occupancies by endogenous DA might affect BP, leading to different excitabilities of neurons. It is known that BP of [11C]SCH23390 is not sensitive to competitive endogenous dopamine even if massive dopamine is released by amphetamine (Abi-Dargham et al., 1999; Chou et al., 1999). However, it is possible that differences in receptor affinity might contribute to differences in DA receptor occupancies, although Farde et al. (1995) reported that variability in D2 receptor affinity is smaller than that in D2 receptor density. Finally, gender and race effects might also be possible. Any generalization should be approached with caution. Notwithstanding these limitations, we expect our finding to contribute to a broadening of the knowledge of the molecular mechanism of functional abnormalities of the amygdala implicated in neuropsychiatric disorders such as schizophrenia (Takahashi et al., 2004), depression (Drevets, 2000) and Parkinson's disease (Tessitore et al., 2002).

References

Abi-Dargham A, Simpson N, Kegeles L, Parsey R, Hwang DR, Anjilvel S, Zea-Ponce Y, Lombardo I, Van Heertum R, Mann JJ, Foged C, Halldin C, Laruelle M (1999) PET studies of binding competition between endogenous dopamine and the D1 radiotracer [^{11}C] NNC 756. Synapse 32:93–109.

Asan E (1998) The catecholaminergic innervation of the rat amygdala. Adv Anat Embryol Cell Biol 142:1–118.

Bissière S, Humeau Y, Lüthi A (2003) Dopamine gates LTP induction in lateral amygdala by suppressing feedforward inhibition. Nat Neurosci 6:587–592.

Brett M, Anton J, Valabregue R, Poline J (2002) Region of interest analysis using the MarsBar toolbox [abstract]. Paper presented at 8th International Conference on Functional Mapping of the Human Brain, Sendai, Japan.

Casanova R, Srikanth R, Baer A, Laurienti PJ, Burdette JH, Hayasaka S, Flowers L, Wood F, Maldjian JA (2007) Biological parametric mapping: a statistical toolbox for multimodality brain image analysis. Neuroimage 34:137–143.

Cervenka S, Pålhagen SE, Comley RA, Panagiotidis G, Cselényi Z, Matthews JC, Lai RY, Halldin C, Farde L (2006) Support for dopaminergic hypoactivity in restless legs syndrome: a PET study on D2-receptor binding. Brain 129:2017–2028.

Chou YH, Karlsson P, Halldin C, Olsson H, Farde L (1999) A PET study of D1-like dopamine receptor ligand binding. Psychopharmacology 146:220–227.

Convit A, McHugh P, Wolf OT, de Leon MJ, Bobinski M, De Santi S, Roche A, Tsui W (1999) MRI volume of the amygdala: a reliable method allowing separation from the hippocampal formation. Psychiatry Res 90:113–123.

de la Mora MP, Gallegos-Cari A, Arizmendi-Garcia Y, Marcellino D, Fuxe K (2009) Role of dopamine receptor mechanisms in the amygdaloid modulation of fear and anxiety: structural and functional analysis. Prog Neurobiol. Advance online publication. Retrieved October 21, 2009. doi:10.1016/j.pneurobio.2009.10.010.

Drevets WC (2000) Functional anatomical abnormalities in limbic and prefrontal cortical structures in major depression. Prog Brain Res 126:413–431.

Farde L, Halldin C, Stone-Elander S, Sedvall G (1987) PET analysis of human dopamine receptor subtypes using 11C-SCH 23390 and 11C-raclopride. Psychopharmacology (Berl) 92:278–284.

Farde L, Hall H, Pauli S, Halldin C (1995) Variability in D2-dopamine receptor density and affinity: a PET study with [^{11}C] raclopride in man. Synapse 20:200–208.

Gunn RN, Lammertsma AA, Hume SP, Cunningham VJ (1997) Parametric imaging of ligand-receptor binding in PET using a simplified reference region model. Neuroimage 6:279–287.

Hariri AR, Mattay VS, Tessitore A, Fera F, Smith WG, Weinberger DR (2002) Dextroamphetamine modulates the response of the human amygdala. Neuropsychopharmacology 27:1036–1040.

Hart AJ, Whalen PJ, Shin LM, McInerney SC, Fischer H, Rauch SL (2000) Differential response in the human amygdala to racial outgroup vs ingroup face stimuli. Neuroreport 11:2351–2355.

Inglis FM, Moghaddam B (1999) Dopaminergic innervation of the amygdala is highly responsive to stress. J Neurochem 72:1088–1094.

Innis RB, Cunningham VJ, Delforge J, Fujita M, Gjedde A, Gunn RN, Holden J, Houle S, Huang SC, Ichise M, Iida H, Ito H, Kimura Y, Koeppe RA, Knudsen GM, Knuuti J, Lammertsma AA, Laruelle M, Logan J, Maguire RP, et al. (2007) Consensus nomenclature for in vivo imaging of reversibly binding radioligands. J Cereb Blood Flow Metab 27:1533–1539.

Ito H, Takahashi H, Arakawa R, Takano H, Suhara T (2008) Normal data-

base of dopaminergic neurotransmission system in human brain measured by positron emission tomography. Neuroimage 39:555–565.
Karlsson S, Nyberg L, Karlsson P, Fischer H, Thilers P, Macdonald S, Brehmer Y, Rieckmann A, Halldin C, Farde L, Backman L (2009) Modulation of striatal dopamine D1 binding by cognitive processing. Neuroimage 48:398–404.
Kates W, Abrams M, Kaufmann W, Breiter S, Reiss A (1997) Reliability and validity of MRI measurement of the amygdala and hippocampus in children with fragile X syndrome. Psychiatry Res 75:31–48.
Kienast T, Hariri AR, Schlagenhauf F, Wrase J, Sterzer P, Buchholz HG, Smolka MN, Grunder G, Cumming P, Kumakura Y, Bartenstein P, Dolan RJ, Heinz A (2008) Dopamine in amygdala gates limbic processing of aversive stimuli in humans. Nat Neurosci 11:1381–1382.
Kröner S, Rosenkranz JA, Grace AA, Barrionuevo G (2005) Dopamine modulates excitability of basolateral amygdala neurons in vitro. J Neurophysiol 93:1598–1610.
Lammertsma AA, Hume SP (1996) Simplified reference tissue model for PET receptor studies. Neuroimage 4:153–158.
LeDoux JE (2000) Emotion circuits in the brain. Annu Rev Neurosci 23:155–184.
Lundqvist D, Flykt A, Ohman A (1998) The Karolinska Directed Emotional Faces. Psychology section, Department of Clinical Neuroscience, Karolinska Institute, Stockholm, Sweden.
Maldjian JA, Laurienti PJ, Kraft RA, Burdette JH (2003) An automated method for neuroanatomic and cytoarchitectonic atlas-based interrogation of fMRI data sets. Neuroimage 19:1233–1239.
Marowsky A, Yanagawa Y, Obata K, Vogt KE (2005) A specialized subclass of interneurons mediates dopaminergic facilitation of amygdala function. Neuron 48:1025–1037.
McNab F, Varrone A, Farde L, Jucaite A, Bystritsky P, Forssberg H, Klingberg T (2009) Changes in cortical dopamine D1 receptor binding associated with cognitive training. Science 323:800–802.
Muller JF, Mascagni F, McDonald AJ (2009) Dopaminergic innervation of pyramidal cells in the rat basolateral amygdala. Brain Struct Funct 213:275–288.
Muly EC, Senyuz M, Khan ZU, Guo JD, Hazra R, Rainnie DG (2009) Distribution of D1 and D5 dopamine receptors in the primate and rat basolateral amygdala. Brain Struct Funct 213:375–393.
Olsson H, Halldin C, Swahn CG, Farde L (1999) Quantification of [11C]FLB 457 binding to extrastriatal dopamine receptors in the human brain. J Cereb Blood Flow Metab 19:1164–1173.
Pezze MA, Feldon J (2004) Mesolimbic dopaminergic pathways in fear conditioning. Prog Neurobiol 74:301–320.
Pinto A, Sesack SR (2008) Ultrastructural analysis of prefrontal cortical inputs to the rat amygdala: spatial relationships to presumed dopamine axons and D1 and D2 receptors. Brain Struct Funct 213:159–175.
Rosenkranz JA, Grace AA (1999) Modulation of basolateral amygdala neuronal firing and afferent drive by dopamine receptor activation in vivo. J Neurosci 19:11027–11039.
Rosenkranz JA, Grace AA (2002) Cellular mechanisms of infralimbic and prelimbic prefrontal cortical inhibition and dopaminergic modulation of basolateral amygdala neurons in vivo. J Neurosci 22:324–337.
Royer S, Martina M, Paré D (1999) An inhibitory interface gates impulse traffic between the input and output stations of the amygdala. J Neurosci 19:10575–10583.
Schwartz CE, Wright CI, Shin LM, Kagan J, Whalen PJ, McMullin KG, Rauch SL (2003) Differential amygdalar response to novel versus newly familiar neutral faces: a functional MRI probe developed for studying inhibited temperament. Biol Psychiatry 53:854–862.
Scibilia RJ, Lachowicz JE, Kilts CD (1992) Topographic nonoverlapping distribution of D1 and D2 dopamine receptors in the amygdaloid nuclear complex of the rat brain. Synapse 11:146–154.
Suhara T, Sudo Y, Okauchi T, Maeda J, Kawabe K, Suzuki K, Okubo Y, Nakashima Y, Ito H, Tanada S, Halldin C, Farde L (1999) Extrastriatal dopamine D2 receptor density and affinity in the human brain measured by 3D PET. Int J Neuropsychopharmacol 2:73–82.
Takahashi H, Koeda M, Oda K, Matsuda T, Matsushima E, Matsuura M, Asai K, Okubo Y (2004) An fMRI study of differential neural response to affective pictures in schizophrenia. Neuroimage 22:1247–1254.
Takahashi H, Kato M, Takano H, Arakawa R, Okumura M, Otsuka T, Kodaka F, Hayashi M, Okubo Y, Ito H, Suhara T (2008) Differential contributions of prefrontal and hippocampal dopamine D1 and D2 receptors in human cognitive functions. J Neurosci 28:12032–12038.
Tessitore A, Hariri AR, Fera F, Smith WG, Chase TN, Hyde TM, Weinberger DR, Mattay VS (2002) Dopamine modulates the response of the human amygdala: a study in Parkinson's disease. J Neurosci 22:9099–9103.
Tzourio-Mazoyer N, Landeau B, Papathanassiou D, Crivello F, Etard O, Delcroix N, Mazoyer B, Joliot M (2002) Automated anatomical labeling of activations in SPM using a macroscopic anatomical parcellation of the MNI MRI single-subject brain. Neuroimage 15:273–289.
Whalen PJ, Davis C, Oler JA, Kim H, Kim J, Neta M (2009) Human amygdala responses to facial expressions of emotions. In: The human amygdala (Whalen PJ, Phelps EA, eds), pp 265–288. New York: Guilford.
Yamamoto R, Ueta Y, Kato N (2007) Dopamine induces a slow afterdepolarization in lateral amygdala neurons. J Neurophysiol 98:984–992.

Behavioral/Systems/Cognitive

Dopamine D_1 Receptors and Nonlinear Probability Weighting in Risky Choice

Hidehiko Takahashi,[1,2,3,4] Hiroshi Matsui,[2] Colin Camerer,[5] Harumasa Takano,[2] Fumitoshi Kodaka,[2] Takashi Ideno,[6] Shigetaka Okubo,[6] Kazuhisa Takemura,[6] Ryosuke Arakawa,[2] Yoko Eguchi,[2] Toshiya Murai,[1] Yoshiro Okubo,[7] Motoichiro Kato,[8] Hiroshi Ito,[2] and Tetsuya Suhara[2]

[1]Department of Psychiatry, Kyoto University Graduate School of Medicine, Kyoto, 606-8507, Japan, [2]Molecular Imaging Center, Department of Molecular Neuroimaging, National Institute of Radiological Sciences, Chiba, 263-8555, Japan, [3]Precursory Research for Embryonic Science and Technology (PRESTO), Japan Science and Technology Agency, Saitama, 332-0012, Japan, [4]Brain Science Institute, Tamagawa University, Tokyo, 194-8610, Japan, [5]Division of Humanities and Social Sciences, California Institute of Technology, Pasadena, California 91125, [6]Department of Psychology, Waseda University, Tokyo, 162-8644, Japan, [7]Department of Neuropsychiatry, Nippon Medical School, Tokyo 113-8603, Japan, and [8]Department of Neuropsychiatry, Keio University School of Medicine, Tokyo 160-8582, Japan

Misestimating risk could lead to disadvantaged choices such as initiation of drug use (or gambling) and transition to regular drug use (or gambling). Although the normative theory in decision-making under risks assumes that people typically take the probability-weighted expectation over possible utilities, experimental studies of choices among risks suggest that outcome probabilities are transformed nonlinearly into subjective decision weights by a nonlinear weighting function that overweights low probabilities and underweights high probabilities. Recent studies have revealed the neurocognitive mechanism of decision-making under risk. However, the role of modulatory neurotransmission in this process remains unclear. Using positron emission tomography, we directly investigated whether dopamine D_1 and D_2 receptors in the brain are associated with transformation of probabilities into decision weights in healthy volunteers. The binding of striatal D_1 receptors is negatively correlated with the degree of nonlinearity of weighting function. Individuals with lower striatal D_1 receptor density showed more pronounced overestimation of low probabilities and underestimation of high probabilities. This finding should contribute to a better understanding of the molecular mechanism of risky choice, and extreme or impaired decision-making observed in drug and gambling addiction.

Introduction

Life is filled with risks. Should I take an umbrella with me this morning? Should I buy car insurance? Which therapy or medicine will improve my health? To answer these questions, and choose, weighting the probability of the possible outcomes is crucial. In particular, misestimating risk could lead to disadvantaged choices such as initiation of drug use (or gambling) and transition to regular drug use (or gambling) (Kreek et al., 2005).

Normative theory in decision-making under risks assumes that people combine probabilities and valuation (utility) of possible outcomes in some way, most typically by taking the probability-weighted expectation over possible utilities. While this expected utility theory (von Neumann and Morgenstern, 1944) is the dominant model, a substantial body of evidence shows that decision makers systematically depart from it (Camerer and Loewenstein, 2004). One type of systematic departure is that subjective weights on probabilities appear to be nonlinear: people often overestimate low probabilities (e.g., playing lotteries) and underestimate high probabilities.

A leading alternative to the expected utility theory is the prospect theory (Tversky and Kahneman, 1992). In the prospect theory, objective probabilities, p, are transformed nonlinearly into decision weights w(p) by a weighting function. Experimental estimates suggest the weighting function is regressive, asymmetric, and inverse S-shaped, crossing the diagonal from above at an inflection point (about 1/3) where p = w(p). In an inverse S-shaped nonlinear weighting function, low probabilities are overweighted and moderate to high probabilities are underweighted. The function neatly explains the typically observed pattern of risk-seeking for low probability gain and risk aversion toward high probability gain.

Risky choice is one of the topics explored in a synthesis of economics and neuroscience called neuroeconomics. Neuroeconomics fMRI studies have demonstrated the neural basis for some other features of the prospect theory such as framing effects and loss aversion (De Martino et al., 2006; Tom et al., 2007). Recently, the neural basis for nonlinear weighting function has also been investigated by fMRI. Hsu et al. (2009) reported that the degree of nonlinearity in the neural response to anticipated re-

Received July 28, 2010; revised Sept. 12, 2010; accepted Oct. 8, 2010.

This study was supported by a consignment expense for Molecular Imaging Program on "Research Base for PET Diagnosis" from the Ministry of Education, Culture, Sports, Science and Technology (MEXT). We thank Katsuyuki Tanimoto and Takahiro Shiraishi for their assistance in performing the PET experiments at the National Institute of Radiological Sciences. We also thank Yoshiko Fukushima of the National Institute of Radiological Sciences for her help as clinical research coordinator.

Correspondence should be addressed to Dr. Hidehiko Takahashi, Department of Psychiatry, Kyoto University Graduate School of Medicine, 54 Shogoin-Kawara-cho, Sakyo-ku, Kyoto, 606-8507, Japan. E-mail: hidehiko@kuhp.kyoto-u.ac.jp.

DOI:10.1523/JNEUROSCI.3933-10.2010

 0270-6474/10/3016567-06$15.00/0

ward in the striatum reflected the nonlinearity parameter as estimated behaviorally.

A deeper question is how modulatory neurotransmission is involved in the central process of decision-making (Trepel et al., 2005; Rangel et al., 2008; Fox and Poldrack, 2009). Investigation of the relationship between the dopamine (DA) system and prospect theory seems promising, considering the fact that DA is linked to risk-seeking behavior (Leyton et al., 2002) and is involved in disrupted decision-making observed in neuropsychiatric disorders such as drug/gambling addiction and Parkinson's disease (Zack and Poulos, 2004; Steeves et al., 2009). Trepel et al. (2005) speculated in a thoughtful review that DA transmission in the striatum might be involved in shaping probability weighting. Using positron emission tomography (PET), we tested this speculation directly by investigating how DA D_1 and D_2 receptors in the brain are associated with transformation of probabilities into decision weights. Phasic DA release occurs during reward and reward-predicting stimuli (Grace, 1991; Schultz, 2007). It is suggested that available striatal D_1 receptors are preferentially stimulated by phasically released DA, whereas low-level baseline tonic DA release is enough for stimulating striatal D_2 receptors (Frank et al., 2007; Schultz, 2007). Because estimating reward cue in our task is considered to induce phasic DA release, we hypothesized that the variability of available D_1 receptors might be more associated with individual differences than that of available D_2 receptors.

Materials and Methods

Subjects

Thirty-six healthy male volunteers (mean age ± SD, 25.2 ± 4.9 years) were studied. They did not meet the criteria for any psychiatric disorder based on unstructured psychiatric screening interviews. None of the controls were taking alcohol at the time, nor did they have a history of psychiatric disorder, significant physical illness, head injury, neurological disorder, or alcohol or drug dependence. Ten subjects were light to moderate cigarette smokers. All subjects were right-handed according to the Edinburgh Handedness Inventory. The vast majority of subjects were university students or graduate school students (three of the participants had finished university and were employed). All subjects underwent MRI to rule out cerebral anatomic abnormalities. After complete explanation of the study, written informed consent was obtained from all subjects, and the study was approved by the Ethics and Radiation Safety Committee of the National Institute of Radiological Sciences, Chiba, Japan.

Procedure

To estimate decision weight, certainty equivalents were determined outside the PET scanner. The behavioral experiment took place 1–2 h before the first PET scans. The procedure was based on the staircase procedure suggested by Tversky and Kahneman (1992), which is the most efficient method for estimating certainty equivalents (Paulus and Frank, 2006; Fox and Poldrack, 2009). A gamble's certainty equivalent is the amount of sure payoff at which a player is indifferent between the sure payoff and the gamble. Participants were presented with options between a gamble and a sure payoff on a computer monitor (supplemental Fig. 1, available at www.jneurosci.org as supplemental material). Gambles were presented that had an objective probability p of paying a known outcome x (and paying zero otherwise). The different combinations of p and x are shown in supplemental Table 1, available at www.jneurosci.org as supplemental material. There were 22 gambles, and half of them were 10,000 yen (~$100) gambles. Because 10,000 yen is the highest-value Japanese paper currency, 11 probabilities were used for 10,000 yen gambles to refine the estimation of weighting function. In each trial, the participants chose between a gamble and a sure payoff. The relative position (left and right) of the two options was randomized to counterbalance for order effects. The subjects were told to make hypothetical rather than actual gambles and were instructed as follows: "Two options for possible monetary gain will be presented to you. Option 1 is a sure payoff and option 2 is a gamble. For example, you will see the guaranteed 6,666 yen on one side of the monitor, and see a gamble in which you have a 50% chance of winning 10,000 yen on the other side. Make a choice between the two options according to your preference by pressing the right or left button. There is no correct answer and no time limit. Once you make a choice, the next options will be presented."

Each time a choice was made between a gamble and a sure payoff in a trial, the amount of a sure payoff in the next trial was adjusted and eight trials per each gamble were iterated to successively narrow the range including the certainty equivalents. The adjustments in the amount of a sure payoff were made in the following manner. The initial range was set between 0 and x (the gamble outcome). The range was divided into thirds. The one-third and the two-thirds intersecting points of the initial range were used as sure payoff options in trials 1 and 2. If the participant accepted the sure option of the two-thirds and rejected that of the one-third in trials 1 and 2, the middle third portion of the initial range was used as a range for trials 3 and 4. If the participant accepted both sure options of the thirds, the lower third part was then used as a range. If the participant rejected both the sure options of the thirds, the upper third part was then used. The new range was again divided into thirds and the same procedure was iterated until the participant completed trial 8. The mean of the final range was used for a certainty equivalent (supplemental Fig. 2, available at www.jneurosci.org as supplemental material). Once a certainty equivalent was estimated for a given gamble, the next gamble was chosen for estimation, and so on. The order of the gambles was randomized across the participants.

Behavioral data estimation

According to the prospect theory, the valuation V of a prospect that pays amount x with probability p is expressed as $v(x, p) = w(p)\,v(x)$, where v is the subjective value of the amount x, and w is the decision weight of the objective probability p. The utility function is usually assumed to be a power function $v(x) = x^{\sigma}$ (results are typically similar to other functions). Although several estimations of the nonlinear probability weighing function have been used in previous experiments (Lattimore et al., 1992; Tversky and Kahneman, 1992; Wu and Gonzalez, 1996), we estimated probability weighting using the one-parameter function derived axiomatically by Prelec (1998), $w(p) = \exp\{-(\ln(1/p))^{\alpha}\}$ with $0 < \alpha < 1$. This function typically fits as well as other functions with one or two parameters (Hsu et al., 2009), and because nonlinearity is fully captured by a single parameter, it is simple to correlate the degree of nonlinearity (α) across individuals with biological measures such as receptor density or fMRI signals (Hsu et al., 2009). This $w(p)$ function has an inverted-S shape with a fixed inflection point at $p = 1/e = 0.37$ (at that point the probability 1/e also receives decision weight 1/e). The parameter α indicates the degree of nonlinearity. A smaller value of α (closer to 0) means a more nonlinear inflected weighting function and a higher value (closer to 1) means a more linear weighting function. At $\alpha = 1$ the function is linear. The weighting function and utility function were estimated by least-squares method.

PET scanning

PET studies were performed on ECAT EXACT HR+ (CTI-Siemens). The system provides 63 planes and a 15.5 cm field of view. To minimize head movement, a head fixation device (Fixster) was used. A transmission scan for attenuation correction was performed using a germanium 68–gallium 68 source. Acquisitions were done in three-dimensional mode with the interplane septa retracted. The first group of 18 subjects (mean age ± SD, 24.7 ± 3.8 years) was studied for both D_1 receptors and extrastriatal D_2 receptors. These 18 subjects came to the PET center twice, once each for the studies of [^{11}C]SCH23390 (R-(+)-7-chloro-8-hydroxy-3-methyl-1-phenyl-2,3,4,5-tetrahydro-1H-3-benzazepine) and [^{11}C]FLB457 ((S)-N-((1-ethyl-2-pyrrolidinyl)methyl)-5-bromo-2,3-dimethoxybenzamide). For evaluation of D_1 receptors, a bolus of 215.9 ± 9.8 MBq of [^{11}C]SCH23390 with specific radioactivities (90.1 ± 38.5 GBq/μmol) was injected intravenously from the antecubital vein with a 20 ml saline flush. The fact that [^{11}C]SCH23390 has high affinity for D_1 receptors (Ekelund et al., 2007), and that D_1 receptors are mod-

erately expressed in the extrastriatal regions (approximately one-fifth of striatal D_1 receptor density) (Ito et al., 2008) leads to good reproducibility of both striatal and extrastriatal [^{11}C]SCH23390 bindings (Hirvonen et al., 2001). Although [^{11}C]SCH23390 is a selective radioligand for D_1 receptors, it has some affinity for $5HT_{2A}$ receptors. However, $5HT_{2A}$ receptor density in the striatum is negligible compared with D_1 receptor density. $5HT_{2A}$ receptor density is never negligible in the extrastriatal regions. Although previous reports in the literature have indicated that [^{11}C]SCH23390 affinity for $5HT_{2A}$ receptors relative to D_1 receptors is negligible, a recent in vivo study reported that approximately one-fourth of the cortical signal of [^{11}C]SCH23390 was due to binding to $5HT_{2A}$ receptors, suggesting that cautious interpretation of the extrastriatal findings regarding this ligand is recommended (Ekelund et al., 2007). For evaluation of extrastriatal D_2 receptors, a bolus of 218.3 ± 13.9 MBq of [^{11}C]FLB457 with high specific radioactivities (238.0 ± 100.8 GBq/μmol) was injected in the same way. [^{11}C]FLB457 has very high affinity for D_2 receptors. It is a selective radioligand for D_2 receptors and has good reproducibility of extrastriatal D_2 bindings (Sudo et al., 2001). Dynamic scans were performed for 60 min for [^{11}C]SCH23390 and 90 min for [^{11}C]FLB457 immediately after the injection. Although [^{11}C]FLB457 accumulates to a high degree in the striatum, striatal data were not evaluated since the duration of the [^{11}C]FLB457 PET study was not sufficient to obtain equilibrium in the striatum (Olsson et al., 1999; Suhara et al., 1999). For radiation safety reason, striatal D_2 receptors were evaluated in the second group of the other 18 subjects [mean age ± SD, 25.7 ± SD 5.9 years]. A bolus of 218.2 ± 10.1MBq of [^{11}C]raclopride with a specific radioactivity of 451.1 ± 154.6 GBq/μmol was injected similarly. [^{11}C]Raclopride is a selective radioligand for D_2 receptors, and has good reproducibility of striatal D_2 bindings (Volkow et al., 1993). Because the density of extrastriatal D_2 receptors is less than one-tenth of striatal D_2 receptors (Ito et al., 2008), [^{11}C]raclopride is suitable for the evaluation of striatal D_2 receptors, but not of extrastriatal D_2 receptors, due to its moderate affinity for D_2 receptors. Dynamic scans were performed for 60 min. All emission scans were reconstructed with a Hanning filter cutoff frequency of 0.4 (full width at half maximum, 7.5 mm). MRI was performed on Gyroscan NT (Philips Medical Systems) (1.5 T). T1-weighted images of the brain were obtained for all subjects. Scan parameters were 1-mm-thick, three-dimensional T1 images with a transverse plane (repetition time/echo time, 19/10 ms; flip angle, 30°; scan matrix, 256 × 256 pixels; field of view, 256 × 256 mm; number of excitations, 1).

Quantification of D_1 and D_2 receptors

Because one subject felt discomfort from the head fixation device during the [^{11}C]FLB457 scan, the scan was discontinued and the data of this subject were excluded from the subsequent analysis. Quantitative analysis was performed using the three-parameter simplified reference tissue model (Lammertsma and Hume, 1996; Olsson et al., 1999). This method is well established for [^{11}C]SCH23390, [^{11}C]FLB457 and [^{11}C]raclopride (Lammertsma and Hume, 1996; Olsson et al., 1999) and is widely used (Aalto et al., 2005; Takahashi et al., 2008; McNab et al., 2009; Takahashi et al., 2010), and it allows us to quantify DA receptors without arterial blood sampling, an invasive and time-consuming procedure. The cerebellum was used as reference region because it has been shown to be almost devoid of D_1 and D2 receptors (Farde et al., 1987; Suhara et al., 1999). The model provides an estimation of the binding potential [$BP_{ND\ (nondisplaceable)}$] (Innis et al., 2007), which is defined by the following equation: $BP_{ND} = k_3/k_4 = f_2\ B_{max}/\{K_d\ [1 + \Sigma_i\ F_i/K_{di}]\}$, where k_3 and k_4 describe the bidirectional exchange of tracer between the free compartment and the compartment representing specific binding, f_2 is the "free fraction" of nonspecifically bound radioligand in brain, B_{max} is the receptor density, K_d is the equilibrium dissociation constant for the radioligand, and F_i and K_{di} are the free concentration and the dissociation constant of competing ligands, respectively (Lammertsma and Hume, 1996). Based on this model, we created parametric images of BP_{ND} using the basis function method (Gunn et al., 1997) to conduct voxelwise statistical parametric mapping (SPM) analysis.

In addition to the SPM analysis, we conducted region-of-interest (ROI) analysis. The tissue concentrations of the radioactivities of [^{11}C]SCH23390, [^{11}C]FLB457 and [^{11}C]raclopride were obtained from anatomically defined ROIs. The individual MRIs were coregistered on [^{11}C]SCH23390, [^{11}C]FLB457 and [^{11}C]raclopride PET images of summated activity for 60, 90 and 60 min, respectively. The ROIs were defined on coregistered MRI with reference to the brain atlas. Given our hypothesis from the previous literature (Hsu et al., 2009), the ROIs were set on the striatum (caudate and putamen). Manual delineation of caudate and putamen ROIs was based on the dorsal caudate and dorsal putamen criteria, respectively, of Mawlawi et al. (2001). The average values of right and left ROIs were used to increase the signal-to-noise ratio for the calculations.

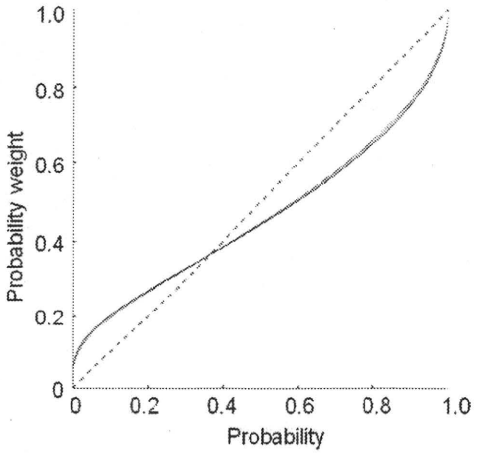

Figure 1. The fitted probability weighting function with the Prelec model. The red line represents the first group (N= 18 subjects) with D_1 receptors and extrastriatal D_2 receptors investigated. The black line is the second group (N= 18 subjects) whose striatal D_2 receptors were investigated.

Statistical analysis

SPM analysis. Parametric images of BP_{ND} of [^{11}C]SCH23390, [^{11}C]FLB457 and [^{11}C]raclopride were analyzed using the SPM2 software package (Wellcome Department of Cognitive Neurology, London, UK) running with MATLAB (MathWorks). Parametric images of BP_{ND} were normalized into MNI (Montreal Neurological Institute) template space. Normalized BP_{ND} images were smoothed with a Gaussian filter to 8 mm full-width half-maximum. Using each of the individual behavioral parameters (α and σ) as covariate, regression analyses with the BP_{ND} images and the covariates were performed. A statistical threshold of $p < 0.05$ corrected for multiple comparisons across the whole brain was used, except for a priori hypothesized regions, which were thresholded at $p < 0.001$ uncorrected ($r > 0.68$) for examination of effect size (only clusters involving 10 or more contiguous voxels are reported). These a priori ROIs included the caudate and putamen.

ROI analysis. Pearson's correlation coefficients between BP_{ND} of [^{11}C]SCH23390 and [^{11}C]raclopride in the ROIs and behavioral parameters (α and σ) were calculated using SPSS software. Because some subjects were smokers, we further calculated partial correlation coefficients between BP_{ND} of [^{11}C]SCH23390 and [^{11}C]raclopride and behavioral parameters to control for the potential influence of smoking (number of cigarettes per day).

Results

In the first group, with D_1 receptors and extrastriatal D_2 receptors investigated, the mean (SD) α of the weighting function and σ of the utility function were 0.58 (0.16) and 0.99 (0.33), respectively. The second group, in which striatal D_2 receptors were investigated, the mean (SD) α and σ were 0.56 (0.19) and 0.98 (0.18), respectively, indicating that the two groups were comparable. Averaged weighting functions and value functions of the two groups are shown in Figure 1 and supplemental Figure 3 (available at www.jneurosci.org as sup-

plemental material), respectively. Normalized parametric images of BP_{ND} of [^{11}C]SCH23390, [^{11}C]raclopride and [^{11}C]FLB457 are shown in Figure 2 A, B, and C, respectively. The mean BP_{ND} values of [^{11}C]SCH23390 in the caudate and putamen were 1.86 ± 0.24 and 2.01 ± 0.22, and those of [^{11}C]raclopride were 3.00 ± 0.32 and 3.61 ± 0.37, respectively. Voxel-by-voxel SPM analysis revealed significant positive correlation ($r > 0.68$, $p < 0.001$) between striatal D_1 receptor binding and the nonlinearity parameter α of weighting function [right striatum, peak (30, −8, −4), 230 voxels; left striatum, peak (−20, −4, 8), 154 voxels] (Fig. 3A). Independent ROI analyses revealed that D_1 receptor binding in the putamen showed a significant correlation with α (Fig. 3B; Table 1), and D_1 receptor binding in the caudate showed a trend level correlation with α (Table 1). That is, people with lower striatal D_1 receptor binding tend to be more risk-seeking for low probability gambles and more risk-averse for high probability gambles. SPM analysis showed that extrastriatal D_1 binding was not correlated with α. SPM and ROI analyses revealed that neither striatal nor extrastriatal D_2 receptor binding was correlated with α. None of [^{11}C]SCH23390, [^{11}C]FLB457 and [^{11}C]raclopride binding was correlated with the power σ of the value function. Correlation analyses with controlling for the potential influence of smoking revealed identical results, indicating that the influence of smoking was minimal. The results of partial correlation analyses of ROIs between behavioral parameters (α and σ) and BP_{ND} values of [^{11}C]SCH23390 and [^{11}C]raclopride in the striatum after controlling for the potential influence of smoking are summarized in supplemental Table 2, available at www.jneurosci.org as supplemental material.

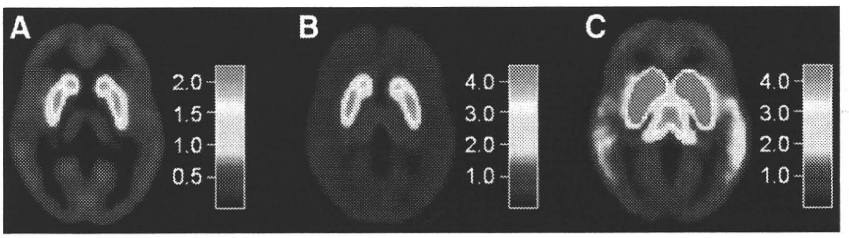

Figure 2. Maps of DA D_1 and D_2 BP, averaged across participants (axial slices at the level of $Z = 0$ of MN coordinates). A, D_1 BP, measured with [^{11}C]SCH23390 (N= 18 subjects). B, Striatal D_2 BP, measured with [^{11}C]raclopride (N= 18 subjects). C, Extrastriatal D_2 BP, measured with [^{11}C]FLB457 (N= 17 subjects). Although [^{11}C]FLB457 accumulates to a high degree in the striatum, striatal data were not evaluated because the duration of the [^{11}C]FLB457 PET study was not sufficient to obtain equilibrium in the striatum. The bar indicates the range of BP.

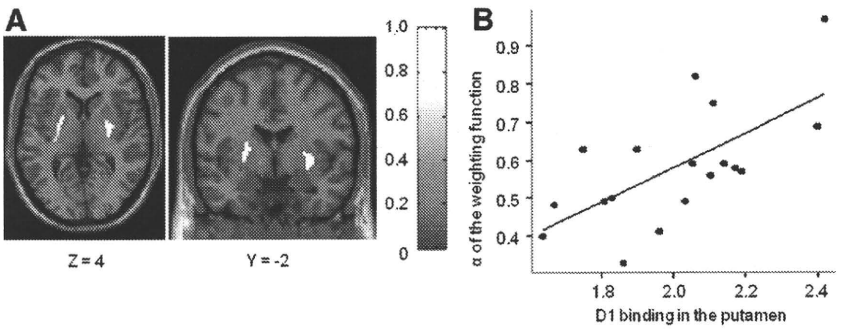

Figure 3. Correlation between nonlinearity of probabilities weighting and D_1 binding in the striatum (N= 18 subjects). A, Image showing regions of correlation between nonlinearity parameter of weighting function and D_1 binding in the striatum. The bar shows the range of the correlation coefficient. B, Plots and regression line of correlation between α (nonlinearity parameter) and binding potential of the putamen ($r = 0.66$, $p = 0.003$).

Table 1. Correlation between behavioral parameters (α and σ) and BP_{ND} values of [^{11}C]SCH23390 (N= 18 subjects) and [^{11}C]raclopride (N= 18 subjects) in the striatum

	α	σ
D_1 receptors		
Caudate	0.011 ($r = 0.582$)	0.717 ($r = 0.092$)
Putamen	0.003* ($r = 0.658$)	0.260 ($r = 0.280$)
D_2 receptors		
Caudate	0.305 ($r = 0.256$)	0.218 ($r = 0.305$)
Putamen	0.242 ($r = 0.291$)	0.122 ($r = 0.378$)

p values (correlation coefficients) are shown. *$p < 0.01$.

Discussion

We provided the first evidence of a relation between striatal D_1 receptor binding and nonlinear probability weighting during decision-making under risk. Based on circumstantial evidence (Kuhnen and Knutson, 2005; Wittmann et al., 2008) and a speculative review (Trepel et al., 2005), it has been suggested that curvature of the weighting function might be modulated by DA transmission. Utilizing a molecular imaging technique, we directly measured the relation between DA receptors and the nonlinearity of weighting function in vivo. Individuals with lower striatal D_1 receptor binding showed more nonlinear probability weighting and more pronounced overestimation of low probabilities and underestimation of high probabilities. Low D_1 receptor binding means that available receptors for phasically released DA are limited. In such case, phasic DA release in response to positive outcomes can stimulate limited D_1 receptors in the striatum. In contrast, low-level baseline tonic DA release is enough for stimulating D_2 receptors (Frank et al., 2007; Schultz, 2007). Therefore, the variability of D_2 receptor binding might have less impact on current behavioral task during which phasic DA release occurs in response to reward cue.

This molecular imaging approach allows us to broaden our understanding of the neurobiological mechanism underlying nonlinear weighting beyond the current knowledge attained by neuroeconomics fMRI. An fMRI study using a value-titration paradigm has shown that differential anterior cingulate activation during estimation of high probabilities relative to low probabilities was positively correlated with Prelec's nonlinearity parameter α across subjects (Paulus and Frank, 2006). Another fMRI study with risks of electric shocks found similar nonlinear response in the caudate/subgenual anterior cingulate (Berns et al., 2008). More recently, Hsu et al. (2009), using a simpler exposure-choice paradigm, demonstrated that Prelec's nonlinearity parameter α was negatively correlated with striatal activity during reward anticipation under risk. That is, people with a greater degree of nonlinearity in striatal activation to anticipated reward tend to overestimate low probabilities (to be risk-seeking) and underestimate high probabilities (to be risk-averse).

Exploring novelty and risk-seeking behavior are, to some extent, desirable and advantageous for the survival and develop-

ment of many species including human (Kelley et al., 2004). Being too risk-averse would lose opportunities to obtain possibly better outcomes. However, excessive risk-seeking may contribute to reckless choices such as initiation of drug use (or gambling) and transition to regular drug use (or gambling) (Kreek et al., 2005). Pathological gambling and drug addiction frequently co-occur, and it is suggested that the neurobiological mechanisms underlying the two conditions overlap (Tamminga and Nestler, 2006; Steeves et al., 2009). In fact, pharmacological therapy for drug addiction has been shown to also be effective when applied to pathological gambling (Tamminga and Nestler, 2006). Animal studies demonstrated that stimulation of D_1 receptors by a selective agonist increased risky choice and blockade of D_1 receptors decreased risky choice in rats. Although D_2 agonist/antagonist showed similar actions, their effects were not as pronounced as those of D_1 agonist/antagonist (St Onge and Floresco, 2009). A human genetic study reported that variants of the gene for D_1 receptors were linked to risky and novelty-seeking behaviors (Comings et al., 1997), although the genes for other subtypes of DA receptors are also linked to those behaviors. More recently, a PET study suggested that reduced D_1 receptor binding may be associated with an increased risk of relapse in drug addiction (Martinez et al., 2009).

The curvature of the weighting function is traditionally explained by the psychophysics of diminishing sensitivity, the idea that sensitivity to changes in probability decreases as probability moves away from the endpoints of 0 and 1 (Tversky and Kahneman, 1992). However, it has also been suggested that emotional responses to gambles influence weighting as well. In particular, the overweighting of low-probability gains may reflect hope of winning and the underweighting of high-probability gains may reflect fear of losing a "near sure thing" (Trepel et al., 2005). One study supportive of this hypothesis found more nonlinear weighting functions for gambles over emotional outcomes (kisses and shocks) than over money (Rottenstreich and Hsee, 2001). In this sense, individuals with lower striatal D_1 binding might be interpreted as showing more "emotional" decision-making.

We used a simple behavioral task with only positive outcomes to estimate weighting function in this study. Any generalization of our findings needs to be approached with caution. We make more complex decisions in the real world where both positive and negative outcomes are possible, and have to pay attention to relative differences in the magnitude of gains and losses. A computational model has suggested that tonic D_2 receptor stimulation in the striatum inhibits response to avoid negative outcomes (Frank et al., 2007), and other neurotransmitters such as serotonin and noradrenaline are thought to be involved in the complex decision-making process (Trepel et al., 2005; Frank et al., 2007; Cools et al., 2008; Doya, 2008). Using behavioral tasks with negative outcomes, future studies to investigate involvements of other neurotransmissions as well as other areas that are related to punishment or negative emotions such as the orbitofrontal cortex, insula and amygdala (Trepel et al., 2005; Pessiglione et al., 2006; Voon et al., 2010) are recommended. Furthermore, our subjects were relatively homogeneous in terms of economic status (the majority were students). Our findings might not be representative of various samples with different background and socioeconomic status. Notwithstanding this limitation, the present study illustrated that molecular imaging can provide a new research direction for neuroeconomics and decision-making studies by more directly investigating the association between striatal DA transmission and nonlinear probability weighting. This approach may shed light on neurotransmission effects on emotional and boundedly rational decision-making in our daily life. At the same time, understanding the molecular mechanism of extreme or impaired decision-making can contribute to the assessment and prevention of drug and gambling addiction and the development of novel pharmacological therapies for those addictions.

References

Aalto S, Brück A, Laine M, Någren K, Rinne J (2005) Frontal and temporal dopamine release during working memory and attention task sin healthy humans: a positron emission tomography study using the high-affinity dopamine D2 receptor ligand [^{11}C] FLB 457. J Neurosci 25:2471–2477.

Berns GS, Capra CM, Chappelow J, Moore S, Noussair C (2008) Nonlinear neurobiological probability weighting functions for aversive outcomes. Neuroimage 39:2047–2057.

Camerer C, Loewenstein G (2004) Behavioral economics: past, present, future. In: Advances in behavioral economics (Camerer C, Loewenstein G, Rabin M, eds), pp 3–51. Princeton: Princeton UP.

Comings D, Gade R, Wu S, Chiu C, Dietz G, Muhleman D, Saucier G, Ferry L, Rosenthal RJ, Lesieur HR, Rugle LJ, MacMurray P (1997) Studies of the potential role of the dopamine D1 receptor gene in addictive behaviors. Mol Psychiatry 2:44–56.

Cools R, Roberts AC, Robbins TW (2008) Serotoninergic regulation of emotional and behavioural control processes. Trends Cogn Sci 12:31–40.

De Martino B, Kumaran D, Seymour B, Dolan RJ (2006) Frames, biases, and rational decision-making in the human brain. Science 313:684–687.

Doya K (2008) Modulators of decision making. Nat Neurosci 11:410–416.

Ekelund J, Slifstein M, Narendran R, Guillin O, Belani H, Guo NN, Hwang Y, Hwang DR, Abi-Dargham A, Laruelle M (2007) In vivo DA D1 receptor selectivity of NNC 112 and SCH 23390. Mol Imaging Biol 9:117–125.

Farde L, Halldin C, Stone-Elander S, Sedvall G (1987) PET analysis of human dopamine receptor subtypes using 11C-SCH 23390 and 11C-raclopride. Psychopharmacology (Berl) 92:278–284.

Fox C, Poldrack R (2009) Prospect theory and the brain. In: Neuroeconomics (Glimcher PW, Camerer C, Fehr E, Poldrack R, eds), pp 145–174. London: Academic.

Frank MJ, Scheres A, Sherman SJ (2007) Understanding decision-making deficits in neurological conditions: insights from models of natural action selection. Philos Trans R Soc Lond B Biol Sci 362:1641–1654.

Grace A (1991) Phasic versus tonic dopamine release and the modulation of dopamine system responsivity: a hypothesis for the etiology of schizophrenia. Neuroscience 41:1–24.

Gunn RN, Lammertsma AA, Hume SP, Cunningham VJ (1997) Parametric imaging of ligand-receptor binding in PET using a simplified reference region model. Neuroimage 6:279–287.

Hirvonen J, Någren K, Kajander J, Hietala J (2001) Measurement of cortical dopamine d1 receptor binding with 11C [SCH23390]: a test-retest analysis. J Cereb Blood Flow Metab 21:1146–1150.

Hsu M, Krajbich I, Zhao C, Camerer CF (2009) Neural response to reward anticipation under risk is nonlinear in probabilities. J Neurosci 29:2231–2237.

Innis RB, Cunningham VJ, Delforge J, Fujita M, Gjedde A, Gunn RN, Holden J, Houle S, Huang SC, Ichise M, Iida H, Ito H, Kimura Y, Koeppe RA, Knudsen GM, Knuuti J, Lammertsma AA, Laruelle M, Logan J, Maguire RP, et al (2007) Consensus nomenclature for in vivo imaging of reversibly binding radioligands. J Cereb Blood Flow Metab 27:1533–1539.

Ito H, Takahashi H, Arakawa R, Takano H, Suhara T (2008) Normal database of dopaminergic neurotransmission system in human brain measured by positron emission tomography. Neuroimage 39:555–565.

Kelley AE, Schochet T, Landry CF (2004) Risk taking and novelty seeking in adolescence: introduction to part I. Ann N Y Acad Sci 1021:27–32.

Kreek MJ, Nielsen DA, Butelman ER, LaForge KS (2005) Genetic influences on impulsivity, risk taking, stress responsivity and vulnerability to drug abuse and addiction. Nat Neurosci 8:1450–1457.

Kuhnen CM, Knutson B (2005) The neural basis of financial risk taking. Neuron 47:763–770.

Lammertsma AA, Hume SP (1996) Simplified reference tissue model for PET receptor studies. Neuroimage 4:153–158.

Lattimore P, Baker J, Witte A (1992) The influence of probability on risky choice: a parametric examination. Behav Organ 17:377–400.

Leyton M, Boileau I, Benkelfat C, Diksic M, Baker G, Dagher A (2002) Amphetamine-induced increases in extracellular dopamine, drug want-

ing, and novelty seeking: a PET/[11C] raclopride study in healthy men. Neuropsychopharmacology 27:1027–1035.
Martinez D, Slifstein M, Narendran R, Foltin RW, Broft A, Hwang DR, Perez A, Abi-Dargham A, Fischman MW, Kleber HD, Laruelle M (2009) Dopamine D1 receptors in cocaine dependence measured with PET and the choice to self-administer cocaine. Neuropsychopharmacology 34:1774–1782.
Mawlawi O, Martinez D, Slifstein M, Broft A, Chatterjee R, Hwang DR, Huang Y, Simpson N, Ngo K, Van Heertum R, Laruelle M (2001) Imaging human mesolimbic dopamine transmission with positron emission tomography: I. accuracy and precision of D2 receptor parameter measurements in ventral striatum. J Cereb Blood Flow Metab 21:1034–1057.
McNab F, Varrone A, Farde L, Jucaite A, Bystritsky P, Forssberg H, Klingberg T (2009) Changes in cortical dopamine D1 receptor binding associated with cognitive training. Science 323:800–802.
Olsson H, Halldin C, Swahn CG, Farde L (1999) Quantification of [11C]FLB 457 binding to extrastriatal dopamine receptors in the human brain. J Cereb Blood Flow Metab 19:1164–1173.
Paulus MP, Frank LR (2006) Anterior cingulate activity modulates nonlinear decision weight function of uncertain prospects. Neuroimage 30:668–677.
Pessiglione M, Seymour B, Flandin G, Dolan RJ, Frith CD (2006) Dopamine-dependent prediction errors underpin reward-seeking behaviour in humans. Nature 442:1042–1045.
Prelec D (1998) The probability weighting function. Econometrica 66:497–527.
Rangel A, Camerer C, Montague PR (2008) A framework for studying the neurobiology of value-based decision making. Nat Rev Neurosci 9:545–556.
Rottenstreich Y, Hsee CK (2001) Money, kisses, and electric shocks: on the affective psychology of risk. Psychol Sci 12:185–190.
Schultz W (2007) Behavioral dopamine signals. Trends Neurosci 30:203–210.
Steeves TD, Miyasaki J, Zurowski M, Lang AE, Pellecchia G, Van Eimeren T, Rusjan P, Houle S, Strafella AP (2009) Increased striatal dopamine release in Parkinsonian patients with pathological gambling: a [11C] raclopride PET study. Brain 132:1376–1385.
St Onge JR, Floresco SB (2009) Dopaminergic modulation of risk-based decision making. Neuropsychopharmacology 34:681–697.
Sudo Y, Suhara T, Inoue M, Ito H, Suzuki K, Saijo T, Halldin C, Farde L (2001) Reproducibility of [11C]FLB 457 binding in extrastriatal regions. Nucl Med Commun 22:1215–1221.
Suhara T, Sudo Y, Okauchi T, Maeda J, Kawabe K, Suzuki K, Okubo Y, Nakashima Y, Ito H, Tanada S, Halldin C, Farde L (1999) Extrastriatal dopamine D2 receptor density and affinity in the human brain measured by 3D PET. Int J Neuropsychopharmacol 2:73–82.
Takahashi H, Kato M, Takano H, Arakawa R, Okumura M, Otsuka T, Kodaka F, Hayashi M, Okubo Y, Ito H, Suhara T (2008) Differential contributions of prefrontal and hippocampal dopamine D1 and D2 receptors in human cognitive functions. J Neurosci 28:12032–12038.
Takahashi H, Takano H, Kodaka F, Arakawa R, Yamada M, Otsuka T, Hirano Y, Kikyo H, Okubo Y, Kato M, Obata T, Ito H, Suhara T (2010) Contribution of dopamine D1 and D2 receptors to amygdala activity in human. J Neurosci 30:3043–3047.
Tamminga CA, Nestler EJ (2006) Pathological gambling: focusing on the addiction, not the activity. Am J Psychiatry 163:180–181.
Tom SM, Fox CR, Trepel C, Poldrack RA (2007) The neural basis of loss aversion in decision-making under risk. Science 315:515–518.
Trepel C, Fox CR, Poldrack RA (2005) Prospect theory on the brain? Toward a cognitive neuroscience of decision under risk. Brain Res Cogn Brain Res 23:34–50.
Tversky A, Kahneman D (1992) Advances in prospect theory: cumulative representation of uncertainty. J Risk Uncertain 5:297–323.
Volkow ND, Fowler JS, Wang GJ, Dewey SL, Schlyer D, MacGregor R, Logan J, Alexoff D, Shea C, Hitzemann R, Angrist B, Wolf AP (1993) Reproducibility of repeated measures of carbon-11-raclopride binding in the human brain. J Nucl Med 34:609–613.
von Neumann J, Morgenstern O (1944) Theory of games and economic behavior. Princeton: Princeton UP.
Voon V, Pessiglione M, Brezing C, Gallea C, Fernandez HH, Dolan RJ, Hallett M (2010) Mechanisms underlying dopamine-mediated reward bias in compulsive behaviors. Neuron 65:135–142.
Wittmann BC, Daw ND, Seymour B, Dolan RJ (2008) Striatal activity underlies novelty-based choice in humans. Neuron 58:967–973.
Wu G, Gonzalez R (1996) Curvature of the probability weighting function. Manage Sci 42:1676–1690.
Zack M, Poulos CX (2004) Amphetamine primes motivation to gamble and gambling-related semantic networks in problem gamblers. Neuropsychopharmacology 29:195–207.